

## Preprocessing: Geocoding of AVIRIS Data using Navigation, Engineering, DEM, and Radar Tracking System Data

Peter Meyer<sup>\*</sup>, Steven A. Larson, Earl G. Hansen, and Klaus I. Itten<sup>1</sup>

Jet Propulsion Laboratory (JPL), California Institute of Technology  
4800 Oak Grove Drive Pasadena, CA 91109, pmeyer@rsl.geogr.unizh.ch

<sup>1</sup> University of Zurich, Remote Sensing Laboratories (RSL), CH-8057 Zurich

### 1. INTRODUCTION

Remotely sensed data have geometric characteristics and representation which depend on the type of the acquisition system used. To correlate such data over large regions with other real world representation tools like conventional maps or Geographic Information Systems (GIS) for verification purposes, or for further treatment within different data sets, a coregistration has to be performed. In addition to the geometric characteristics of the sensor there are two other dominating factors which affect the geometry: the stability of the platform and the topography. There are two basic approaches for a geometric correction on a pixel-by-pixel basis: (a) A parametric approach using the location of the airplane and inertial navigation system data to simulate the observation geometry and (b) a non-parametric approach using tie points or ground control points (Itten and Meyer, 1993). It is well known that the non-parametric approach is not reliable enough for the unstable flight conditions of airborne systems, and is not satisfying in areas with significant topography, e.g. mountains and hills. The present work describes a parametric preprocessing procedure which corrects effects of flight line and attitude variation as well as topographic influences and is described in more detail by Meyer (1993c).

### 2. BASIS OF THE STUDY

*Test site and image data:* The area "Zug-Buochserhorn" is the standard test site of the Remote Sensing Laboratories, University of Zurich-Irchel in Central Switzerland. The region was covered by the AVIRIS flight #910705, run 6 of the NASA MAC Europe'91 campaign providing a data swath with an average nominal pixel size of about 18m. The first scene, Zug, represents a hilly area with highest elevation differences of about 600m and slopes with typical angles between 15° and 60°. The second scene, Rigi, is an example of mountainous terrain with elevation differences of about 1400m and maximum slope angles up to 90°.

*AVIRIS auxiliary data:* The quality assessment for the actual data set is described in detail in Meyer et al. (1993b). The current work uses the navigation data roll, pitch, and true heading (generated through the ER-2 Inertial Navigation System) and the roll and pitch of the AVIRIS instrument's precision gyros.

*Digital elevation model (DEM):* The test area is covered by the two digital models (DHM-25) Zug and Rigi generated by the Swiss Federal Office of Topography<sup>\*\*</sup>. They have a resolution of 25m in i and j direction and of 0.10 m in elevation e with an average error in elevation of 2.2m±1.0m for model Zug, and 4.4m±1.8m for Rigi.

*ADOUR conical radar tracking system:* The ground-based immobile tracking radar system ADOUR is a dual antenna, dual frequency radar with a conical scan tracking system operated by the Swiss Air Force (Thomson-CSF, 1987). For the

<sup>\*</sup> now at: University of Zurich-Irchel, Remote Sensing Laboratories, Winterthurerstrasse 190, CH-8057 Zurich

<sup>\*\*</sup>DEM data courtesy: Swiss Federal Office of Topography, July 05, 1993

current approach the three parameters latitude  $x$ , longitude  $y$ , and altitude  $z$  are used. The systematic error for elevation and azimuth is  $\pm 0.2\text{mrad}$  and  $\pm 7\text{m}$  for distance with an update interval of 0.2 second.

*Ground reference information:* A forest map was generated by scanning the green (forest) plate of the Swiss Topographic Map, scale 1:25,000, edition 1987 at  $50\ \mu\text{m}$  with an Optronics 5040 Scanner. The average cartographic accuracy is about 5.0 m. A shoreline map was produced by digitizing the same map in an ARC/Info using a digitizing tablet. The average (theoretical) accuracy is  $\pm 8.0\text{m}$ .

### 3. METHOD

Figure 1 gives an overview of the core task for the new method for geocoding AVIRIS data. The basic goal is to reconstruct for every pixel the geometric situation at the time it was acquired with AVIRIS. This includes three major aspects. The first considers the flight line and attitude of the ER-2 aircraft, the second reconstructs the current observation geometry and the third treats the situation on the surface. This approach includes the three different coordinate systems  $(c,r)$  for the raw file, longitude  $x$ , latitude  $y$ , and altitude  $z$  together with roll  $\omega$ , pitch  $\phi$ , and true heading  $\chi$  for the observation geometry and  $(i,j, e_{i,j})$  for the DEM.

*Flight line and attitude of the ER-2 aircraft:* The  $x,y$ , and  $z$  of the aircraft need to be known as a first step. For the 1991 European flight the information results from an unaided LTN90-116 INS navigation system with a position accuracy of 0.9 nmi/h (Perrin, 1993). These data are not accurate enough for the current approach. Therefore, ADOUR data are used as an alternative. The description of the attitude of the aircraft is based on the  $\chi$  from the navigation data and the  $\omega$  and  $\phi$  from the instrument data.

*Current observation geometry:* The basic idea is shown in Figure 2 and described in more detail by Larson et al. (1994). The effort is to obtain the underlying surface out of the well-known location (=flight line) and the current attitude of the aircraft. The position vector  $X_{c,r}$  represents the location of pixel  $(c,r)$  in the aircraft coordinate system  $(x,y,z)$  at the instant the pixel was acquired by the instrument and for the ideal case where  $\omega = \phi = \chi = 0^\circ$ :

$$X_{c,r} = \left( \left( \left[ \tan \left( \left( c - \frac{\max P - 1}{2} \right) \frac{FOV}{\max P} \right) \right] Z_{x,y} \right) \right) Z_{x,y}, \quad (1)$$

where  $c$  = pixel number of pixel  $(c,r)$  within line  $r$  of the raw image,  $\max P$  = maximum number of pixels per line (614),  $FOV$  = Field of View (in rad), and  $Z_{x,y}$  = altitude of ER-2 for the current  $x$  and  $y$ . The pixelwise calculation of the actual pointing direction includes correction of the panoramic distortion. The vector  $X_{c,r}$  is modified by rotations about the  $\omega$ ,  $\phi$ , and  $\chi$  axis (vector  $X_{c,r}'''$ , Figure 2). The transformed position vector  $X_{c,r}'''$  is computed as follows:

$$X_{c,r}''' = \begin{pmatrix} 1 & -\chi & -\phi \\ \chi & 1 & -\omega \\ \phi & \omega & 1 \end{pmatrix} X_{c,r}. \quad (2)$$

*Situation on surface:* The topography causes a shift in the apparent pixel location, and affects the pixel size. The goal is now to find the intersection between the pixel location vector  $X_{i,j}'''$  and the surface of the DEM. Within the neighborhood

around the transformed pixel location vector  $X''_{i,j}$ , a test vector  $X^*_{i,j}$  is searched for, which converges to  $X''_{i,j}$ .

$$X^*_{i,j} = \begin{pmatrix} i - i_{Nadir} \\ j - j_{Nadir} \\ \frac{(Z_{x,y} - e_{i,j})}{v} \end{pmatrix}, \quad (3)$$

where  $i_{Nadir}$  = i-coordinate of the true nadir point,  $j_{Nadir}$  = j-coordinate of the true nadir point,  $e_{i,j}$  = elevation of the test point at position (i,j), and  $Z_{x,y}$  = altitude of ER-2 for the current x and y. To allow for a more precise selection of the corresponding surface point, the DEM oversampled to a grid size of 6m is used. To define the intersection point on the surface, the normalized dot product of  $X^*_{i,j}$  and  $X''_{i,j}$  is calculated. The vector  $X^*_{i,j}$  best representing  $X''_{i,j}$  is that for which the dot product DP has the smallest difference from 1. To represent the pixel size dependent on the topography, the four corner points (6m grid size) of every pixel are separately calculated. To prevent changes to the radiometric characteristics, the original value is selected by an improved extraction algorithm during the resampling to an 18m grid size, thereby eliminating the need to interpolate the values.

#### 4. DISCUSSION AND OUTLOOK

There are currently no well-established methods of quantitatively assessing the success of a geocoding process. Visual inspection provides useful information, but cannot be used to intercompare methods. Statistical results based on residual calculation of single ground control points allow only a local error assessment.

For the discussion, the Rigi scene is selected because of the more challenging topography. Figure 3 shows bands 13, 18, and 28 of the geocoded image overlaid by the scanned forested areas (green line) and digitized shoreline (blue line). The enlarged areas are selected dependent on their aspect and slope angle. In general, the results show a good correspondence between the geocoded image and the map for all existing topographical locations. A few locations show minor miscorrespondence. These problems are almost always restricted to single pixels and no general tendency can be recognized. The errors may result from changes in reality between the time the aerial photographs (which are the basis for the topographic maps) were acquired (1987) and the AVIRIS data acquisition, and on the fact that maps are the result of a generalization while AVIRIS displays every occurrence within its resolution characteristics. Figure 3B demonstrates another problem of the ground reference information. While the lower regions of the forested slope correspond perfectly, the AVIRIS image extends significantly the forest area on the upper limits. This "misregistration" is based on the problem of the determination of the forest border along the timber line and its representation in the forest map through symbolic point signatures which are suppressed through the scanning process. Figure 3D and Figure 3E portray areas with rapidly changing slope angles. The blue shoreline proves for subarea (D) and the green forest line for subarea (E) the good correspondence. The additional verification calculates the average deviation of the geocoded image compared with the forest and lake map for checkpoints. Lines 1 and 2 of Table 1 indicate the results of this test and confirm the visual validation. No systematic deviation was found. To double-check the performance of the new parametric

approach, scene Rigi was geocoded using the improved, non-parametric rubber-sheet approach (Itten and Meyer, 1993). Table 2 (line 3) presents the result for the improved rubber-sheet approach and shows the better performance of the parametric solution.

The datasets Zug and especially Rigi need georadiometric corrections. Atmospheric corrections using radiative transfer models like MODTRAN-2a (Green et al., 1993) as well as a compensation for the slope-aspect-dependent illumination difference (Meyer et al., 1993a) should complete the preprocessing of the sensor, system and scene related effects of the current data set.

The whole procedure was implemented using the IDL (Interactive Data Language, a proprietary programming language, Research System Inc., 1993).

## 5. ACKNOWLEDGMENTS

The first author would like to thank the Swiss Research Foundation and NASA for supporting the project and K.I. Itten (RSL), G. Vane, R. O. Green, and E. G. Hansen (JPL) for providing special assistance. The support of the NASA Ames Research Center, the Swiss Air Force, and Litton, Aero Products, Woodlands, CA is gratefully acknowledged. Thanks for technical assistance go to R.O. Green, T. G. Chrien, A. T. Murray, H. I. Novack, M. Solis, P. J. Nielsen, J. J. Genofsky, and C. Chovit (JPL) as well as to T. Kellenberger, M. Schaepman, S. Sandmeier, C. Ehrler, E. H. Meier, S. Veraguth, U. Kurer, and D. Schlaepfer (RSL).

The research described in this paper was carried out at the Jet Propulsion Laboratory, California Institute of Technology, and was sponsored by the Swiss Research Foundation, Project No. 8220-33290.

## 6. REFERENCES

- Green, R. O., J. E. Conel, T. G. Chrien (1993), Correction of AVIRIS Radiance to Reflectance using MODTRAN-2, in *Proc. International Society for Optical Engineering (SPIE) 1937*, Orlando, FL (in press).
- Itten, K. I., and P. Meyer (1993), Georadiometric correction of TM-Data of mountainous forest areas, *IEEE Transactions on Geoscience and Remote Sensing* (in press).
- Larson, S., P. Meyer, and E. G. Hansen (1994), Topographical and Geometric Correction of Remote Sensing Image Data using Dead Reckoning, *IEEE Transactions on Geoscience and Remote Sensing* (in preparation).
- Meyer, P., K. I. Itten, T. Kellenberger, R. Leu, and S. Sandmeier (1993a), Radiometric and Geometric Correction of TM-Data of Mountainous Forest Areas, *ISPRS Journal of Photogrammetry and Remote Sensing: 48* (in press).
- Meyer, P., R. O. Green, and T. G. Chrien (1993b), Extraction of Auxiliary Data from AVIRIS Distribution Tape for Spectral, Radiometric, and Geometric Quality Assessment, in *Proc. of the Fourth Annual JPL Airborne Geoscience Workshop*, Washington, D.C. Published by Jet Propulsion Laboratory, Pasadena, California (this volume).
- Meyer, P. (1993c), A Parametric Approach for the Geocoding of Airborne Visible/Infrared Imaging Spectrometer (AVIRIS) Data in Rugged Terrain, *Remote Sensing of Environment* (submitted).
- Perrin, D. (1993), Personal communication (fax Jan 28, 1993).
- Research Systems, Inc.<sup>®</sup> (1993), IDL User's Guide, Version 3.0, Boulder, CO.
- Thomson-CSF (1987), Radar ADOUR, Modernisation télémétrie et codage, Tome I.

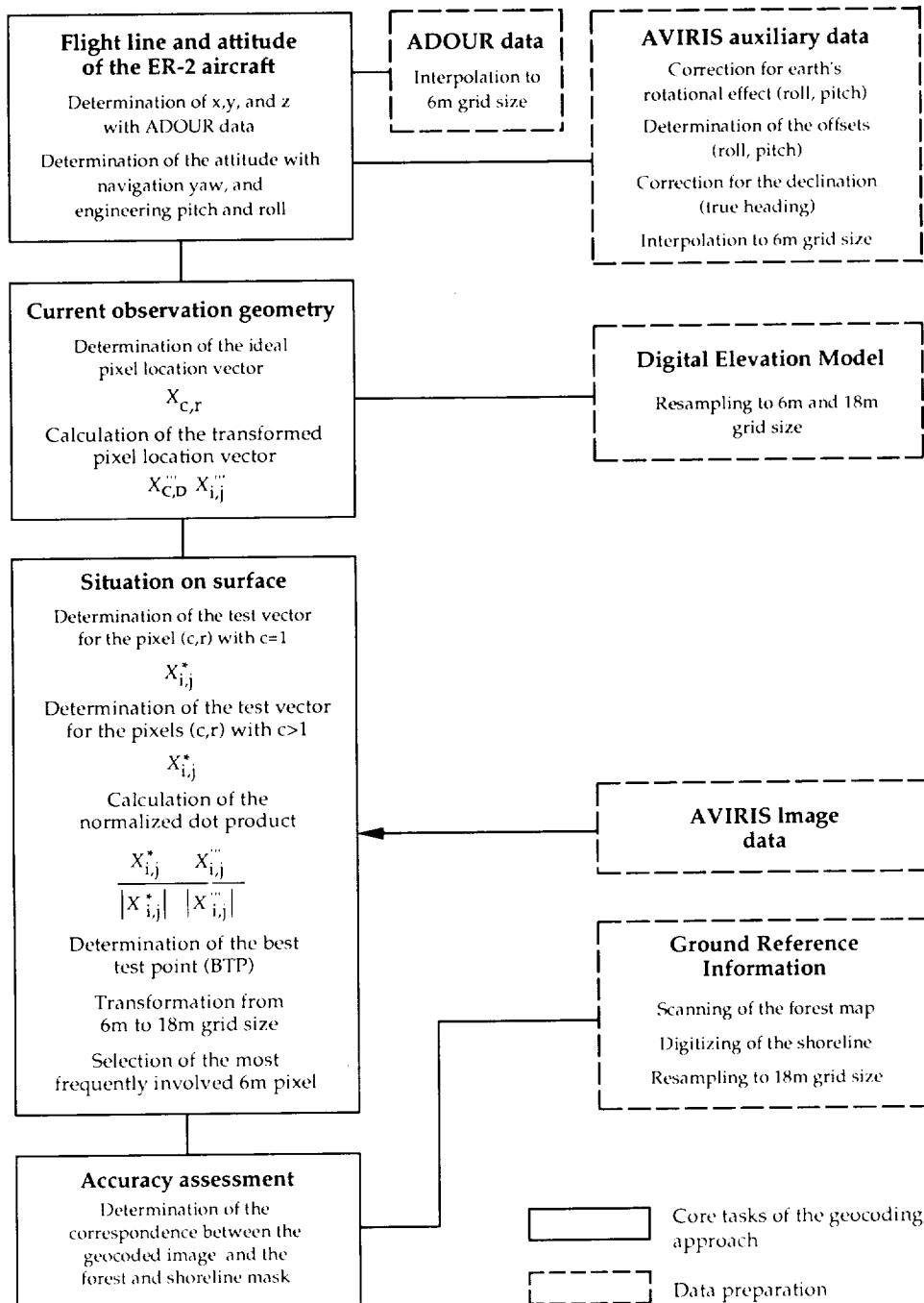


Figure 1: Overview of the data preparation and core tasks of the geocoding approach, where x=latitude, y=longitude, z=altitude of the airplane, and c=column and r=row of the raw file.

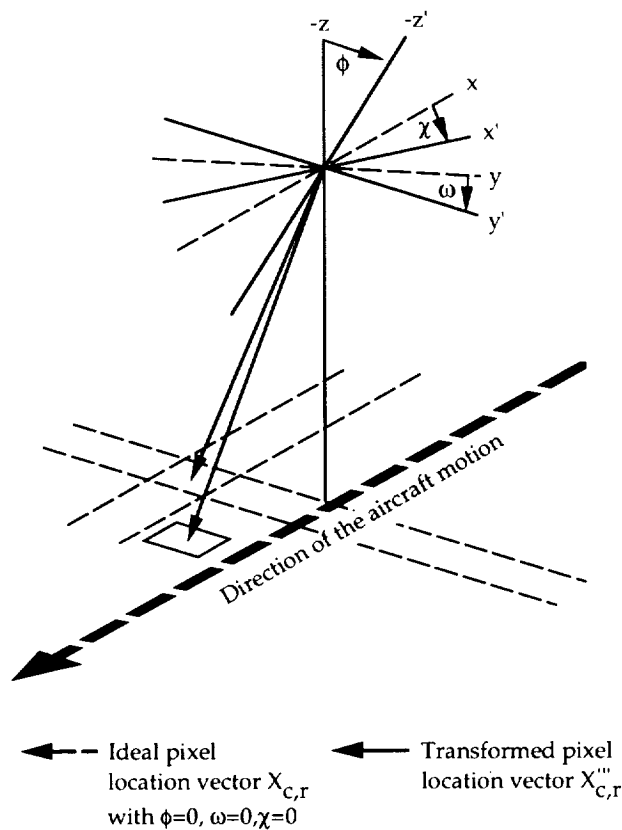


Figure 2: Principal outline of the observation geometry to calculate the transformed pixel location vector where  $\phi$ =pitch,  $\omega$ =roll, and  $\chi$ =true heading, and  $x,y,z$  defining the coordinate axis for the ideal pixel location vector and  $x',y',z'$  for the transformed pixel location vector.

Figure 3 (Slide 7): (A) shows the composite rendered on the digital elevation model with tags (B-E) for the location of the enlarged subareas of the horizontal (non-rendered) composite. (B)-(E) show zoom-up ( $\approx$  factor 5) parts with different aspect and slope angles.

Table 1: Result of the quantitative effort for the comparison between the geocoded images and the forest map with the RMS for the east-west direction (i) and north-south direction (j) of the digital elevation model. The check points used for the non-parametric approach for scene Rigi are a selection from the entire number of points used for the parametric approach.

	No. of checkpoints	RMS for i-direction	RMS for j-direction
Scene Zug (parametric approach)	186	0.07 pixel	0.19 pixel
Scene Rigi (parametric approach)	309	0.12 pixel	0.09 pixel
Scene Rigi (non-parametric approach)	249	3.57 pixel	1.37 pixel